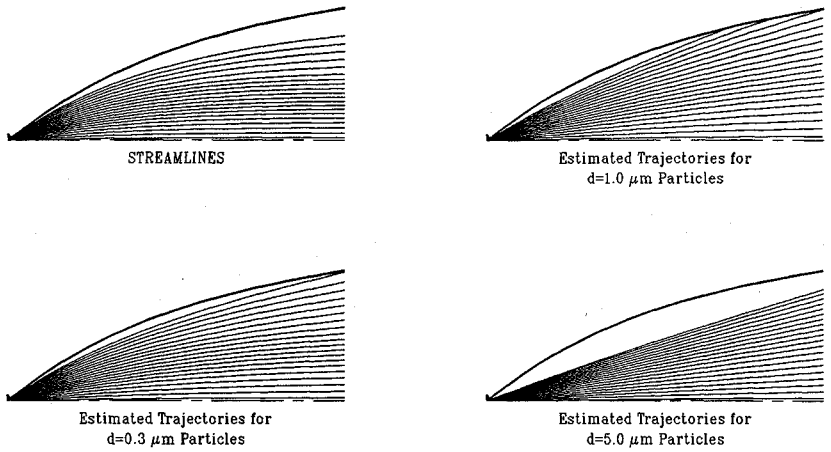

Fig. 2 Computed streamlines and particle trajectories through the nozzle.

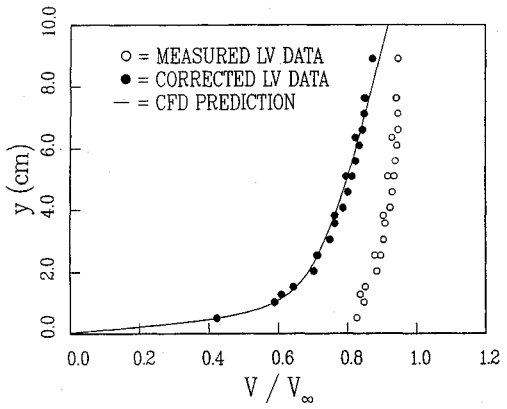

Fig. 3 Original and corrected velocity profiles for 1.0-μm alumina particles.

The raw and corrected velocity profiles for the 1.0-μm alumina are shown in Fig. 3. The velocity profile from the computational solution is plotted for comparison. In contrast to the 0.3-μm profile, the 1.0-μm-seed corrected profile shape agrees extremely well with the CFD prediction, because of the reasonably accurate modeling of the particle size. The excellent agreement between the corrected measurements and the computational prediction show that the particle velocity lag bias may be accounted for in hypersonic flows with very weak gradients.

Conclusions

The feasibility of LV measurements at Mach 12 has been examined for the Aeromechanics Division Twenty-Inch Hypersonic Wind Tunnel. Velocity measurements using nominally 0.3- and 1.0-μm alumina seed particles reveal the following: 1) seed particles of various diameters have different response characteristics, which result in particle-size-dependent velocity profiles, even within the relatively mild flow gradients encountered within the shear layer; 2) corrected velocity profiles for the nominally 1.0-μm alumina agree extremely well with the CFD prediction. Velocity profiles for the nominally 0.3-μm particles do not show as good agreement, because of contamination by at least one additional particle size. Although the current study has shown that accurate shear-layer profiles may be obtained by correcting experimental data with a numerically estimated velocity lag, the poor particle response to even the mildest gradients in the flowfield indicates that LV measurements using alumina seed larger than 0.3 μm in diameter are not a suitable diagnostic for the Mach 12 facility.

References

[1]Schmisseur, J. D., and Maurice, M. S., "An Investigation of Laser Velocimetry Particle Behavior within Flow Structures at Mach 12," AIAA Paper 94-0668, Jan. 1994.

[2]Molten, R. G., "Results from a Flowfield Survey of the Air Force Wright Aeronautical Laboratory Twenty Inch Hypersonic Wind Tunnel," Air Force Wright Aeronautical Lab., AFWAL-TM-88-187-FIMG, Wright Patterson AFB, OH, Sept. 1988.

[3]Ames Research Staff, "Equations, Tables and Charts for Compressible Flow," NACA Report 1135, 1953.

[4]Keyes, F. G., "A Summary of Viscosity and Heat Conduction Data for He, Ar, H_2, O_2, N_2, CO, CO_2, H_2O, and Air," *Transactions of the American Society of Mechanical Engineers*, Vol. 73, July 1951, pp. 589–596.

[5]Trolier, J. W., "Hypersonic Nozzle Flow Simulation Task 3," Science Applications International Corporation, SAIC/VF-88:004, Wayne, PA, Dec. 1988.

[6]Maurice, M. S., "Quantitative Laser Velocimetry Measurements in the Hypersonic Regime by the Integration of Experimental and Computational Analysis," AIAA Paper 93-0089, Jan. 1993.

Calculation of Wing-Alone Aerodynamics to High Angles of Attack

F. G. Moore* and R. M. McInville†
Naval Surface Warfare Center, Dahlgren, Virginia 22448-5100

Introduction

THE recent version of the NSWCDD Aeroprediction Code (AP93) released to the public[1–3] was limited in angle of attack (AOA) to about 30 deg because the wing-alone, wing-body, and body-wing interference aerodynamics were developed only up to about 30-deg AOA. In some cases, the accuracy degraded at an AOA of 25 deg. One reason for this degradation was the second-order accuracy of the method derived for the wing-alone solution. While this method gave much better estimates of wing aerodynamics than the linear theory of the 1981 version of the Aeroprediction Code (AP81) above α of about 10 deg, it still failed for AOA greater than about 30 deg.

To understand why the second order method fails at $\alpha \geq 30$ deg, refer to Fig. 1. Figure 1 examines the physical characteristics of the wing-alone normal force C_{Nw} and normal-force coefficient derivative $C_{N\alpha}$ as a function of aspect ratio (AR) and Mach number (M_∞). As seen in Fig. 1, at low to moderate values of the AR, typical

Received April 1, 1994; revision received Sept. 9, 1994; accepted for publication Sept. 12, 1994. This paper is declared a work of the U.S. Government and is not subject to copyright protection in the United States.

*Senior Aerodynamicist, Code G04, Weapons Systems Department, Dahlgren Division, 17320 Dahlgren Road. Associate Fellow AIAA.

†Aerospace Engineer, Code G23, Aeromechanics Branch, Dahlgren Division, 17320 Dahlgren Road.

REGION	$C_{N\alpha}$ CHARACTERISTICS
A	• CAN BE INCREASING OR DECREASING DEPENDING ON AR • POINT OF INFLECTION MAY OCCUR ABOVE α = 25 deg
B	• POINT OF INFLECTION TYPICALLY OCCURS FOR LOW TO MODERATE AR. NO POINT OF INFLECTION FOR HIGHER AR
C	• $C_{N\alpha}$ TYPICALLY DECREASING • $C_{N\alpha}$ = 0 AT α = 90 deg
D	• MIRROR IMAGE OF REGIONS A, B, C

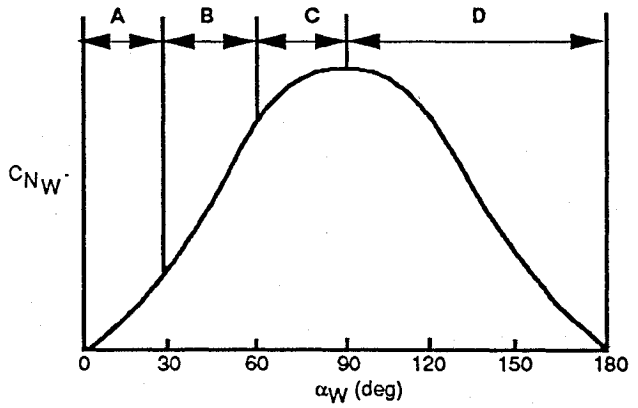

Fig. 1 Qualitative characteristics of normal-force coefficient of wings alone at all AOAs.

of those used for most missiles, $C_{N\alpha}$ will typically increase as the AOA increases. This increase is larger with the smaller-AR wings, where the linear lift term is smallest [$C_{N\alpha}$ approaches $(\pi/2)$AR]. At high AR, where the linear lift term approaches its two-dimensional value of 2π, the nonlinear lift with AOA greater than about 10 to 15 deg is typically negative. In all cases, there is a noticeable effect of compressibility for large values of M_∞. These two effects can be modeled reasonably well up to α of about 30 deg with a second-order technique. However, only the high-AR wing-alone lift curves could be successfully modeled with a second-order technique above α of 25 to 30 deg. That is because the low- to moderate-AR planforms have a point of inflection where the slope of the C_N-versus-α curve changes sign. As a result, a second-order technique for estimating the wing-alone normal force will fail for these planforms at higher AOA, and higher-order mathematical models must be examined.

In examining the literature for high-AOA semiempirical methods for wing-alone aerodynamics, Fidler and Bateman[4] developed a fourth-order method in α as an improvement on the second-order method that was used in Refs. 1–3. However, the method of Ref. 4 had two fundamental problems. First, the authors used the wing-alone estimate of normal force and normal-force coefficient derivative at AOA 0, 90, and 180 deg. In using these conditions, inaccuracies occurred away from the endpoints due to a lack of information between α = 0 and 90 deg and between α = 90 and 180 deg. The second problem with Ref. 4's method was that it was developed in the early 1970s when not many wing-alone data were available; hence, it was limited in Mach number and AR.

While Ref. 4's method does not give as accurate and generically applicable a technique as desired, it is the correct general approach for high-AOA wing-alone solutions. The method developed in this paper is similar but much more accurate and robust. As such, it is believed to be the first accurate and robust wing-alone semiempirical method for estimating normal force over the entire AOA and Mach-number range. Therefore, it is the first step in extending the AP93 code above AOA of 30 deg.

Analysis

The nonlinear wing-alone normal-force coefficient model of Ref. 1 is

$$C_{Nw} = \left[(C_{N\alpha})_{\alpha=0}\,\alpha_w + K_1 \sin^2 \alpha_w\right]\frac{A_w}{A_{\text{ref}}} \tag{1}$$

$(C_{N\alpha})_{\alpha=0}$ of Eq. (1) is based primarily on linearized theories, and K_1 is an empirically derived constant that depends on M_∞, the taper ratio λ, the AR, and the Mach number M_N normal to the wing planforms. As already discussed, this method works quite well up to α_w = 25 to 30 deg. However, beyond that, a higher-order prediction method is needed for many wing planforms. A more accurate method to estimate C_{Nw} is given by

$$C_{Nw} = a_0 + a_1\alpha_w + a_2\alpha_w^2 + a_3\alpha_w^3 + a_4\alpha_w^4 \tag{2}$$

The quantity α_w in both Eqs. (1) and (2) is defined as the AOA of the unperturbed freestream on the wing itself. That is,

$$\alpha_w = |\alpha + \delta| \tag{3}$$

where δ is the wing deflection. Here, only positive AOAs (α_w) are considered, since it is assumed that the missile wing planforms have no camber, and as a result the normal force at a negative AOA is simply the negative of that at the corresponding positive value.

To predict the wing-alone normal force using Eq. (2) now requires that five constants be evaluated, versus three for Eq. (1). Since there are five constants, five independent equations or conditions are needed. The first condition has already been mentioned. That is, most missile lifting surface planforms are symmetric and have zero camber. As a result, $(C_N)_{\alpha=0}$ = 0, and therefore, from Eq. (2), $a_0 = 0$.

Secondly, we will assume that at α = 0, $C_{N\alpha}$ can be estimated accurately enough by linearized theories. Once again, Eq. (2) yields $a_1 = (C_{N\alpha})_{\alpha=0}$. These values of $(C_{N\alpha})_{\alpha=0}$ are already available in the AP93 and are known to give reasonably accurate results for planforms where the thickness is not too large and the AOA is fairly small.

To determine the remaining three conditions, several alternatives are available. The first alternative is to take advantage of the fact that at α = 90 deg, $C_{N\alpha}$ = 0, since C_{Nw} is a maximum at α = 90 deg. Using this condition and two values of C_{Nw} at two different AOAs, the remaining three constants can be determined. The question here is which two AOAs to use. One set that warrants consideration is α_1 = 30 deg and α_2 = 60 deg, since this divides the AOA range up into equal 30-deg increments where the conditions are defined for evaluating the constants a_i.

Examining Fig. 1, it is seen that a fairly strong nonlinearity occurs for α < 30 deg for low-AR wings. Hence, an argument could be made that a lower value of α would be more appropriate than α_1 = 30 deg. For example, the pairs of values α_1 = 20 deg, α_2 = 60 deg and α_1 = 20 deg, α_2 = 45 deg can be used for comparison with α_1 = 30 deg, α_2 = 60 deg.

A fourth option for defining the three remaining constants using the fourth-order Eq. (2) is to use three values of α rather than using two values of α and the condition that $C_{N\alpha}$ = 0 at α = 90 deg. In view of the strong nonlinearity below α = 30 deg for low-AR configurations and the fact $\alpha \leq 30$ deg is the most important part of the AOA range, values of α_1 = 15 deg, α_2 = 30 deg, and α_3 = 60 deg seem appropriate. To provide more equal spacing between α_1 = 15 deg and α_3 = 60 deg, yet focus more on the α = 0–30-deg range, another alternative for α_2 is 35 deg. Above α = 60 deg, approximate equations can be used to extend the C_{Nw} from α = 60 deg to α = 90 deg.

Each of the five alternatives outlined in the previous discussion for computing the three coefficients a_2, a_3, and a_4 of Eq. (2) requires three different sets of equations. These equations have been derived and are given in Ref. 5. Detailed tables comparing these five methods are also given in Ref. 5. For brevity, only the mathematical model of the best of the five methods and tabulated accuracy results comparing the five methods will be presented. That method is the one where three data points are chosen for normal-force computations at α = 15, 35, and 60 deg.

Table 1 Wing-alone model for $\alpha_w > 60$ deg when three data sets for C_{Nw} are chosen

For $M_\infty \geq 2.0$; 60 deg $< \alpha_w \leq 90$ deg:

$$C_{Nw} = (C_{Nw})_{\alpha_w=60\text{ deg}} \left(\frac{\sin \alpha_w}{\sin 60\text{ deg}} \right)$$

For $M_\infty \leq 1.2$; 60 deg $< \alpha_w \leq 90$ deg:

$$C_{Nw} = (C_{Nw})_{\alpha_w=60\text{ deg}} \left(\frac{\sin \alpha_w}{\sin 60\text{ deg}} \right)^{1/3}$$

For $1.2 < M_\infty < 2.0$; 60 deg $< \alpha_w \leq 90$ deg:
extrapolate between values at $M = 1.2$ and 2.0:

$$C_{Nw} = (C_{Nw})_{M=1.2} + [(C_{Nw})_{M=2.0} - (C_{Nw})_{M=1.2}] \frac{M - 1.2}{0.8}$$

The equations that define the coefficients a_2, a_3, and a_4 are[5]

$$a_2 = 34.044(C_N)_{\alpha=15\text{ deg}} - 4.824(C_N)_{\alpha=35\text{ deg}} + 0.426(C_N)_{\alpha=60\text{ deg}} - 6.412a_1 \quad (4)$$

$$a_3 = -88.240(C_N)_{\alpha=15\text{ deg}} + 23.032(C_N)_{\alpha=35\text{ deg}} - 2.322(C_N)_{\alpha=60\text{ deg}} + 11.464a_1 \quad (5)$$

$$a_4 = 53.219(C_N)_{\alpha=15\text{ deg}} - 17.595(C_N)_{\alpha=35\text{ deg}} + 2.661(C_N)_{\alpha=60\text{ deg}} - 5.971a_1 \quad (6)$$

Here $(C_N)_{\alpha=15\text{ deg}}$, $(C_N)_{\alpha=35\text{ deg}}$, and $(C_N)_{\alpha=60\text{ deg}}$ are the values of the normal-force coefficient that are obtained from the data bases of Refs. 6–8. These tables are given in Ref. 5. Again a_1 is the slope of the linear normal-force curve, available in the AP93,[1–3] primarily from linear theory.

Two other points need to be considered before completion of the analysis section. These have to do with the normal force on the wing alone for $\alpha > 90$ deg for any of the methods discussed previously, and with the normal force on the wing alone for the methods where three values of α were selected for determining the coefficients a_2, a_3, and a_4. For the latter problem, no condition was taken for $C_{N\alpha}$ at $\alpha = 90$ deg, and the maximum AOA chosen for the normal-force tables was at $\alpha = 60$ deg. Hence, one might expect erroneous results for 60 deg $< \alpha \leq 90$ deg in some cases. To remedy this situation, some approximate formulas have been developed for this AOA range that are more consistent with the trends of the data in Refs. 6–8. Since data are available for most wing planforms at $\alpha = 60$ deg, the formulas use this value and largely extrapolate from it. The overall method is given in Table 1.

The other problem mentioned is that for $\alpha > 90$ deg. Then we define an AOA α^* by

$$\alpha = \pi/2 + \alpha^* \quad (7)$$

where α^* is the excess of α over 90 deg. Then, from symmetry considerations,

$$(C_{Nw})_{\alpha=\pi/2+\alpha^*} = (C_{Nw})_{\alpha=\pi/2-\alpha^*} \quad (8)$$

A summary of the wing-alone fourth-order estimation process is as follows:

1) Use tables from Ref. 5 to compute the values of C_{N1}, C_{N2}, and C_{N3} for the wing in question and at the Mach number of interest. Linear interpolation between the tables should be adequate.

2) Compute the value of a_1 from the aeroprediction code or another method as desired.

3) Use Eqs. (4–6) to compute a_2, a_3, and a_4.

4) Knowing a_0, a_1, a_2, a_3, and a_4, use Eq. (2) to compute C_{Nw} of the wing for the given total AOA of the wing.

5) If 60 deg $< \alpha_w <$ 90 deg, use the equations in Table 1 to compute the value of C_{Nw} at appropriate α and M.

6) If $\alpha_w > 90$ deg, use Eq. (8) to compute the value of C_{Nw}.

Table 2 Global errors for C_{Nw}

Method	Error, %
AP93	6.04(—)
AP3060	6.72(5.94)
AP2045	4.73(5.58)
AP2060	4.97(4.52)
AP153060	3.38(3.79)
AP153560	3.87(3.59)

Results and Discussion

Detailed comparisons of the five methods for computing the coefficients a_i are given in Ref. 5. Only one summary table of these five methods will be presented here. These results are given by Table 2 in terms of an overall comparison of the global performance of the methods. For purposes of identification, AP93 refers to the second-order technique used in the current version of the NSWCDD Aeroprediction Code. AP3060, AP2045, and AP2060 refer to the fourth-order schemes that rely on only two reference values of C_{Nw} for their solutions. As the designations imply, AP3060 uses reference points of 30 and 60 deg, AP2045 uses reference points of 20 and 45 deg, and AP2060 uses reference points of 20 and 60 deg. The fourth-order schemes using three reference points of 15, 30, and 60 deg or 15, 35, and 60 deg are identified as AP153060 and AP153560, respectively. The numbers without parentheses were obtained by considering α only up to 30 deg. Since AP93 results are valid only within this range, it is these values that offer a comparison of the new techniques with the old. In instances where error values are shown in parentheses, comparison data were available up to $\alpha = 60$ deg, and these numbers represent the averages over the entire AOA range from 10 to 60 deg. Also, each line in Table 2 represents data for several Mach numbers ($M = 0.8, 1.2, 2.0, 4.5$), taper ratios ($\lambda = 0, 0.5, 1.0$), and ARs (0.5, 1.0, 2.0, 4.0).

As can be seen from the table, the new techniques do a good job in most cases, but the two-reference-point formulations (AP3060, AP2045, AP2060) give results inferior to the three-reference-point methods (AP153060, AP153560). Also, all of the fourth-order methods, except AP3060, perform better than the current AP93 second-order approach in the 10–30-deg AOA range. The AP153060 method gives the best results, followed closely by AP153560. Over the extended AOA range from 10 to 60 deg, AP153560 gives the best results, as indicated by the numbers in parentheses. Since AP153560 also reduced some large errors in the AOA range near 40 deg, it was chosen as the method for integration into the Aeroprediction Code.

Further validation of the new method on configurations outside the data base and on total missile configurations is still needed. This will be accomplished after the next phase of the work is completed, which will extend the various interference factors of the work in Refs. 1–3 to $\alpha > 30$ deg.

Even with the anomalies just discussed, the new fourth-order method gives improvement in wing-alone normal-force prediction of about 35% over the second-order method (see Table 2) in the AOA range 0 to 30 deg. Moreover, the average error in the AOA range 0 to 60 deg is even lower than in the range 0 to 30 deg. Both these average errors are less than 4% using the AP153560 method.

Summary

A new fourth-order semiempirical method has been developed to estimate wing-alone aerodynamics at all Mach numbers and AOAs. The method utilizes the linearized theory approaches of the AP93 along with wing-alone data bases to evaluate constants needed in the fourth-order equation. On comparing the new technique with data and the AP93, we find that the new method not only gave aerodynamics over the entire AOA range but also was more accurate, on average, than the AP93 method in the range of $0 \leq \alpha \leq 30$ deg.

In deriving the new method, many extrapolations were needed at low Mach numbers and high ARs, where either data were lacking or the data available had questionable accuracy. As a result, additional accurate wing-alone wind-tunnel data are needed for 1) AR = 4.0, $\lambda = 0, 1.0$, at all Mach numbers, and 2) $M < 1.5$, $\alpha > 30$ deg, at all aspect ratios. These additional data would allow the present

method to be fine-tuned and eliminate most of the extrapolations in the technique.

Acknowledgments

Appreciation is expressed to Tom Loftus, Craig Porter, and Robin Staton, who manage the technology programs that supported this task, and to Dave Siegel, who sponsored the work.

References

[1]Moore, F. G., Hymer, T. C., and McInville, R. M., "Improved Aeroprediction Code: Part I—Summary of New Methods and Comparison with Experiment," Naval Surface Warfare Center Dahlgren Division, NSWCDD/TR-93/91, Dahlgren, VA, May 1993.

[2]Moore, F. G., McInville, R. M., and Hymer, T. C., "Improved Aeroprediction Code: Part II—Computer Program User's Guide and Listing," Naval Surface Warfare Center Dahlgren Division, NSWCDD/TR-93/241, Dahlgren, VA, Aug. 1993.

[3]Moore, F. G., Hymer, T. C., and McInville, R. M., "A Planar Nonlinear Missile Aeroprediction Code for all Mach Numbers," AIAA Paper 94-0026, Jan. 1994.

[4]Fidler, J. E., and Bateman, M. C., "Aerodynamic Methods for High Incidence Missile Design," *Journal of Spacecraft and Rockets*, Vol. 12, No. 3, 1975, pp. 162–168.

[5]Moore, F. G., and McInville, R. M., "A New Method for Calculating Wing-Alone Aerodynamics to Angle of Attack 180 deg," Naval Surface Warfare Center Dahlgren Division, NSWCDD/TR-94/3, Dahlgren, VA, March 1994.

[6]Stallings, R. L., Jr., and Lamb, M., "Wing-Alone Aerodynamic Characteristics for High Angles of Attack at Supersonic Speeds," NASA Technical Paper 1889, July 1981.

[7]Baker, W. B., Jr., "Static Aerodynamic Characteristics of a Series of Generalized Slender Bodies with and without Fins at Mach Numbers from 0.6 to 3.0 and Angles of Attack from 0 to 180 deg," Arnold Engineering Development Center, TR-75-124, Vols. I and II, Tullahoma, TN, May 1976.

[8]Nielsen, J. N., Hemsch, M. J., and Smith, C. A., "A Preliminary Method for Calculating the Aerodynamic Characteristics of Cruciform Missiles to High Angles of Attack Including Effects of Roll Angle and Control Deflections," Office of Naval Research, Report ONR-CR215-216, 4F, Arlington, VA, Nov. 1977.

Identification of an Error in the Distribution of the NASA Model AP-8 MIN

Daniel Heynderickx*
Belgisch Instituut voor Ruimte-Aëronomie (BIRA/IASB), Ringlaan 3, B-1180 Brussells, Belgium
and
Alexey Beliaev†
Moscow State University, Moscow 119899, Russia

Introduction

THE NASA trapped radiation models AP-8 and AE-8, for protons and electrons, respectively,[1] are widely used to describe the particle fluxes in the Earth's trapped radiation belts. For some years now, the proton models that are available on line at the National Space Science Data Center (NSSDC) have been reduced versions of these models, called AP-8 MIC and AP-8 MAC. The full models AP-8 MIN and AP-8 MAX are only available on specific request.

Recently, we tracked down an error in the previously distributed version of the model AP-8 MIN. This error can be corrected in a straightforward way, so that AP-8 MIN can be reinstated.

Received June 7, 1994; revision received Sept. 6, 1994; accepted for publication Sept. 30, 1994.

*Assistant, Mathematische Aëronomie, Fundamentele Dynamica. Member AIAA.

†Scientist, Space Physics, Skobeltsyn Institute of Nuclear Physics.

The second section of this paper contains a description of the NASA trapped-particle models. In the third section, we relate how we identified the error in the AP-8 MIN data file and how it can be corrected. The fourth section is devoted to a comparison of the compressed models AP-8 MIC and AP-8 MAC with the full models AP-8 MIN and AP-8 MAX.

Description of the NASA Models AP-8 and AE-8

The proton models[2] AP-8 MIN and AP-8 MAX and the electron models[3] AE-8 MIN and AE-8 MAX are the last in a series of trapped radiation models developed by NASA since the 1960s.[4] They consist of integer arrays of scaled integral particle fluxes as a function of the particle energy E and of the magnetic coordinates B/B_0 and L, where B is the magnetic field at a given location, L is McIlwain's[5] parameter, and $B_0 = M/L^3$, with $M = 0.311653$ Gauss R_E^3, the value of the geomagnetic moment used by McIlwain[5] in his definition of L (L is expressed in units of Earth radii R_E). The logical organization of the model files is described by Vette.[3]

There are two versions of each model, denoted by MIN and MAX, valid for conditions of solar minimum and maximum, respectively. Otherwise, the models are static with epochs 1964 and 1970. AE-8 MIN/MAX and AP-8 MIN should be accessed with Jensen and Cain's[6] geomagnetic field model, which is not time-dependent. For AP-8 MAX one should use the GSFC 12/66 model,[7] updated to 1970. Using other field models may result in considerable errors on the predicted fluxes.[8]

The trapped-radiation models are distributed[1] with a subroutine called TRARA that interpolates between grid points in E, B/B_0, L. Daly and Evans[9] found that with TRARA there are problems when interpolating between L values at low altitude. They derived a new interpolation scheme in terms of the quantity $\varphi = \arcsin[(B - B_0)/(B_c - B_0)]$, where B_c is the magnetic field strength at the atmospheric cutoff. In this way, much smoother flux contours are obtained. All calculations presented here made use of this new interpolation method.

The models originally were distributed in Fortran BLOCK DATA format. Since computer memory was limited at the time of the release of the models, compressed versions of the proton models AP-8 MIN and AP-8 MAX were made available. These versions were denoted by AP-8 MIC and AP-8 MAC and require less than half the storage space of the full versions. The software package RADBELT distributed by the National Space Science Data Center (NSSDC)[1] uses the AP-8 MIC and AP-8 MAC flux maps.

Description and Correction of a Problem in AP-8 MIN

At BIRA/IASB, both AP-8 MIN/MAX and AP-8 MIC/MAC are implemented. Recently, while performing calculations with AP-8 MIN, we found a discrepancy in our copy of this model. Figure 1 shows the integral flux spectrum for $L = 2$, $B/B_0 = 1$, obtained with AP-8 MIN. Clearly, there is a discrepancy in the model around 0.6 MeV. When we repeated our calculations with AP-8 MIC, we found no errors. Upon closer investigation, we found that AP-8 MIC and AP-8 MIN differ substantially in the region bounded by $0.5 \leq E \leq 0.8$ (in MeV) and $1.4 \leq L \leq 2.7$, where the differences in fluxes reach three orders of magnitude.

We found the same error in a copy of the AP-8 MIN map we received from A. Vampola (private communication), and also in a new copy that we requested from NSSDC. On visual inspection, we noticed that two lines in the seven-column data file were misplaced, i.e. lines 842–843 were placed after line 798 (the corrupted section of the data file is reproduced in Fig. 2). Line 798 is located in the energy block for 0.6 MeV and contains the beginning of the data block for $L = 1.4$ [the problem with AP-8 MIN was also traced to this region in E and L by H. Evans (private communication)]. Consequently, the wrong values for the increment in B/B_0 are read in this L block. In addition, the value 115 is now read as the length of the next L block, and 263 for the length of the block after that. By an outrageous coincidence, the next value read after the 378 erroneous ones actually falls on the beginning of the L block for $L = 2.7$, at line number 855. Since lines 842–843 have been passed by now, the rest of the file is read correctly. Without this coincidence, the error could have spread through the whole of the remainder of the model